

Intrinsic complications in the analysis of optical-pump, terahertz probe experiments

Han-Kwang Nienhuys and Villy Sundström*
*Department of Chemical Physics, Chemical Center,
Lund University, Box 124, 221 00 Lund, Sweden*
(Dated: April 3, 2005 (revised manuscript))

A general formalism is presented for the interpretation of experiments in which a laser pulse (or pump pulse) creates charge carriers that are subsequently probed by a broadband THz pulse (or probe pulse). The time-dependence of the sample properties is described in terms of the conductivity $\sigma(\omega, \tau)$, where the dependence on frequency ω describes the intrinsic properties of the charge carriers and the dependence on pump-probe delay τ describes their population dynamics. It is shown that there are significant complications in obtaining this quantity from experimental data for τ values comparable to the charge carrier response time. Also, in transient THz absorption experiments, fast dynamics in the measured signals may be observed that do not necessarily reflect sample dynamics.

PACS numbers: 07.57.Pt, 72.20.Jv

I. INTRODUCTION

Terahertz (THz) spectroscopy involves radiation with frequencies most often in the range 0.3–3 THz, corresponding to wavelengths of 100 to 1000 μm , or photon energies of 1 to 10 meV. In this paper, we concentrate on the use of THz spectroscopy to study the behavior of charge carriers in the condensed phase. There are several advantages of using THz radiation for that purpose. First, due to the small photon energies, THz radiation is not likely to excite electrons and holes. However, it can generate an electrical current in a sample. Moreover, scattering of charge carriers typically happen on a timescale of femtoseconds to picoseconds, which one can expect to see as features in the absorption spectrum at THz frequencies. Finally, it is possible to generate broadband THz pulses with a duration of a few cycles, which has created the possibility to do optical-pump, terahertz-probe (OPTP) spectroscopy. For a comprehensive overview of the field of THz spectroscopy, see Ref. 1, and, more focused on OPTP spectroscopy, Ref. 2.

In an OPTP experiment, an ultrashort laser pulse excites a sample, typically creating or exciting charge carriers. Subsequently, these photoexcited charge carriers are probed by a broadband pulse of terahertz radiation. This is similar to more conventional optical pump-probe spectroscopy, apart from the fact that it is possible to measure the full time dependence of the electrical field of the THz probe pulse, instead of only its energy or energy spectrum. By means of Fourier analysis, the full complex absorption spectrum can be obtained, which describes both amplitude change and the phase shift as a function of frequency. This conveys more information than the energy spectrum alone. Moreover, it is possible to observe dynamics occurring on a timescale as fast as 0.1 ps even though the THz pulse has a duration of several picoseconds.^{3–13} However, as we will show in this paper, it is by no means trivial to relate the observed fast dynamics in the signal to the underlying material properties such as the charge-carrier density and the single-carrier response.

In a full OPTP experiment, the time profile $E(t)$ of a THz probe pulse that has passed through a sample is measured as a function of pump-probe delay τ . A few studies have treated the issue of interpreting such experimental data from a theoretical point of view. Kindt and Schmuttenmaer¹⁴ describe the response of polar molecules in liquid solution in terms of the susceptibility $\Delta\chi(t, \tau)$. Also in terms of susceptibility is a study by Nemeč and co-workers,¹⁵ which proposes to describe the sample properties in terms of $\Delta\chi(\omega, \omega')$, where both t and τ are transformed to the frequency domains. However, it is much more intuitive to describe the charge carrier response in a sample in terms of its frequency-dependent electrical conductivity $\sigma(\omega)$ rather than the susceptibility. Indeed, a number of experimental studies describe the sample in terms of $\sigma(\omega)$ in steady-state conditions^{16,17} or in terms of $\sigma(\omega, \tau)$ in combination with photoexcitation.^{3,4,6,10,13} In an older theoretical study, Vengurlekar and Jha¹⁸ describe the sample properties with a time-dependent conductivity spectrum $\sigma(\tau, \omega)$, but they focus mostly on processes occurring in GaAs.

The aim of this paper is to provide a solid description of the optical pump-THz probe technique in terms of a time- and frequency-dependent conductivity $\sigma(\tau, \omega)$. First, we will give a short introduction about the straightforward steady-state case. Then we will proceed with introducing a mathematical formalism that is needed to describe the interaction of a THz pulse with a sample that has time-dependent properties in a meaningful manner. With this formalism, we will consider the problem of obtaining those properties from experimental data. This will turn out to be more complicated than previously assumed.

II. MEASURING THE STEADY-STATE CONDUCTIVITY

Similarly to other authors,^{3,5,9,10,13,16} we describe the properties of the sample in terms of the complex conductivity spectrum $\sigma(\omega)$, that relates the electric current

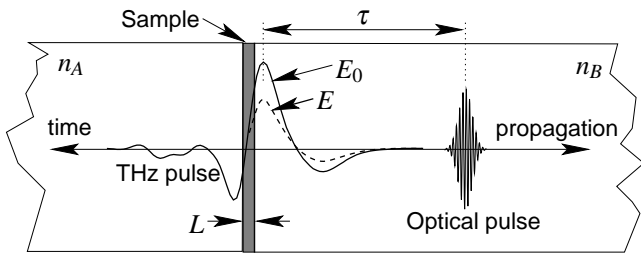


FIG. 1: Definition of the experimental parameters in an optical-pump, THz probe experiment. The sample is a slab with thickness L , surrounded by media with refractive indexes n_A and n_B at THz frequencies. The sample is excited by an optical pulse, followed by a THz pulse $E_0(t)$ with a time delay τ . After undergoing absorption by the excited sample, the THz field amplitude changes to $E(t)$.

density to an applied electric field with amplitude E_0 at frequency ω , according to

$$J(t) = \Re[\sigma(\omega)E_0e^{-i\omega t}]. \quad (1)$$

A standard model for electrical conductivity is the Drude model,¹⁹ in which charge carriers can move freely, although their motion is subject to damping with a time constant τ_D . This leads to the expression

$$\sigma(\omega) = \frac{\sigma_0}{1 - i\omega\tau_D}, \quad (2)$$

where σ_0 depends, among other things, on the concentration of charge carriers and their effective mass. Note that the minus sign in the denominator of Eq. (2) is dependent on the chosen sign convention for the exponent in Eq. (1).

The conductivity of a sample can be obtained experimentally by comparing the reference THz pulse field $E_0(t)$ that passed through a non-excited or blanco sample to the field $E(t)$ that passed through an excited sample. For given refractive indexes n_A and n_B of the surrounding materials, and a sample thickness L as shown in Fig. 1, it can be derived (see Appendix A) that

$$J(t) = -\frac{\epsilon_0 c(n_A + n_B)}{L}[E(t) - E_0(t)], \quad (3)$$

where ϵ_0 is the dielectric constant of vacuum and c the speed of light. It can be interpreted as that the electric current in the sample emits radiation that interferes with the incoming radiation E_0 that passes through the sample. This emitted radiation need not be in phase with the incoming radiation: the sample can continue radiating *after* the THz pulse has passed through. Note that this equation holds for thin samples; Appendix A also discusses to what extent it may be applied to thick samples.

Having obtained $J(t)$, we can define the Fourier operator

$$\mathcal{F}\{f(t)\}(\omega) \equiv \int_{-\infty}^{\infty} f(t)e^{i\omega t} dt, \quad (4)$$

which we use to evaluate the frequency-domain conductivity

$$\sigma(\omega) = \frac{\mathcal{F}\{J(t)\}(\omega)}{\mathcal{F}\{E_0(t)\}(\omega)}, \quad (5)$$

following its definition in Eq. (1). We have assumed that the differential signal $\Delta E \equiv E - E_0$ is small compared to E_0 . Also, we assumed that the conductivity is not dependent on the depth in the sample. This assumption is not correct if the conductivity is the result of an optical excitation and the optical penetration is comparable to or smaller than the sample thickness. In that case, the true conductivity is a function $\sigma(\omega, z)$ of the depth z , while the conductivity as evaluated above is the average,

$$\sigma(\omega) = \int_0^L \sigma(\omega, z) dz. \quad (6)$$

We would like to stress that the main point of this paper is to show how a time-dependent conductivity fundamentally affects the measured signals, even if complications such as sample size are ignored.

III. FORMALISM FOR TIME-DEPENDENT CONDUCTIVITY

In an optical-pump, terahertz probe experiment, an ultrashort optical pulse generates charge carriers, which subsequently disappear due to processes such as recombination and trapping. The THz probe, that passes through the sample at a time delay τ is affected by the charge carriers. The aim of such an experiments is to obtain a conductivity spectrum $\sigma(\omega, \tau)$ as a function of time τ after excitation. By choosing this form, one implicitly assumes that the measured conductivity consists of the summed contributions of various charge carrier species, each with a number density n_k and single-particle conductivity $\varsigma_k(\omega)$, or

$$\sigma(\omega, \tau) = n_1(\tau)\varsigma_1(\omega) + n_2(\tau)\varsigma_2(\omega) + \dots \quad (7)$$

This is analogous to the case in transient-absorption spectroscopy, where the absorbance change can be written as the sum of contributions by various species. However, this analogy is far from complete. The charge carriers may be generated and recombine within a fraction of a picosecond, i.e., a fraction of an oscillation period at 1 THz. Does it make sense to define the conductivity at 1 THz for such a short-lived species? The answer is yes, but only if the concept of conductivity is interpreted in a strictly defined manner, as we will show now.

First, we realize that the conductivity spectrum is the Fourier transform of the the impulse response current density, i.e. the current density that would result from a δ -pulsed THz field, and that can be split further into a charge carrier density N and a single-particle impulse response $j_0(t)$. In the Drude model, $j_0(t)$ is an exponentially decaying function. (Note that this means that

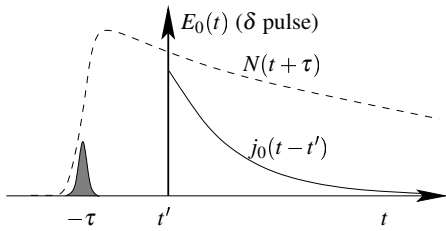


FIG. 2: The single-particle current response j_0 and charge carrier density N for an excitation pulse at time $-\tau$ and a THz δ -pulse at time t' .

the sample response continues even when the THz pulse has already passed through.) We assume a δ -pulsed THz field (we will generalize for arbitrary THz pulse shapes later on) at time t' and an excitation pulse at time $-\tau$. The charge carrier density at time t is given by $N(t + \tau)$ and the single-particle current by $j_0(t - t')$, as shown in Fig. 2.

One might now write the total current after a THz δ -pulse as $j(t, t', \tau) = N(t + \tau)j_0(t - t')$, such that the current decreases due to both the intrinsic properties of the charge carrier and the decreasing population. However, charge carriers that are created at $t > t'$, for example if the excitation pulse appears after the THz δ -pulse, will not contribute to an increasing current since they never felt the driving electrical field at t' . Imagine, for example, that there is only one free electron in the sample that is accelerated by the THz pulse and thus carries a small current. If, directly after the THz pulse, 10^{15} new charge carriers are created, the current will of course not increase with a factor 10^{15} , but will rather still be carried by the original one electron. Hence, a decrease in N for $t > t'$ should decrease the current, while an increase in N should have no effect at all. A consistent description requires elaborate bookkeeping of which part of the density $N(t)$ was already present at $t = t'$, and which part was created later on. Obviously, this is inconvenient. However, this description may be used if no new charge carriers are created for $t > t'$.

A better way to describe the current, still assuming a THz δ pulse at $t = t'$, is to incorporate the decay in population into the single-particle impulse response. This means that we no longer make a mathematical distinction between the two effects that lead to a decaying electrical current, one being friction acting on the charge-carrier motion and the other being the charge carriers disappearing altogether due to, e.g., electron-hole recombination. Hence, we define a new single-particle impulse response

$$\hat{j}_0(t) = j_0(t)p(t), \quad (8)$$

where $p(t)$ is the probability that a charge carrier disappears within a time t . For example, $j_0(t) \propto \exp(-t/\tau_D)$ and $p(t) = \exp(-t/\tau_R)$, where τ_D and τ_R are the Drude damping time and the charge-carrier recombination time, respectively. Now, the current response after a THz δ

pulse at $t = t'$ is given by

$$j(t, t', \tau) = N(t' + \tau)\hat{j}_0(t - t'), \quad (9)$$

regardless of whether $N(t)$ increases or decreases with time.

Summarizing, there are two ways to view conductivity, the *intrinsic-conductivity* picture and the *conductivity-with-population* picture, in terms of $j_0(t)$ and $\hat{j}_0(t)$, respectively, or in the frequency domain,

$$\zeta(\omega) \equiv \mathcal{F}\{j_0(t)\}(\omega), \quad (10a)$$

$$\hat{\zeta}(\omega) \equiv \mathcal{F}\{\hat{j}_0(t)\}(\omega). \quad (10b)$$

Only the conductivity-with-population picture can adequately describe systems with a growing charge carrier density. The reason that we mention both is that in published time-resolved THz conductivity studies, the intrinsic-conductivity picture seems to be assumed implicitly. Moreover, as we will see, the latter has certain advantages when experimental data is analyzed.

In an experiment, the THz pulse is not a δ -pulse but rather a time-varying field $E_0(t)$, which can be several picoseconds in duration. We can, in either the intrinsic-conductivity or the conductivity-with-population picture, write the total current J as a convolution

$$J(t, \tau) = N(t + \tau)[E_0(t) * j_0(t)], \quad (11a)$$

$$J(t, \tau) = [E_0(t)N(t + \tau)] * \hat{j}_0(t). \quad (11b)$$

Due to the complications discussed above, Eq. (11a) is only correct if $\tau \gg 0$, i.e. there is no overlap between the pump and the THz pulse (\gg indicates that the difference should be larger than the durations of the pump and probe pulses). Finally, we remark that we assume that there is only one charge-carrier species. However, the equations can easily be generalized for an arbitrary number of species.

IV. OBTAINING TIME-VARYING CONDUCTIVITY FROM EXPERIMENTS

In an experiment, the current density $J(t, \tau)$ can be obtained directly through Eq. (3), and Eqs. (11a) and (11b) show how this measurable quantity is related to the unknown N and \hat{j}_0 and the known THz pulse E_0 . In the remainder of this section, we will try to transform the measured quantity J into a quantity that is more directly related to the physically relevant properties N and \hat{j}_0 . In the time-varying case, this is a bit more involved than in the steady-state case [Eq. (5)]. The first step is to apply the time-shift operation

$$J_T(t, \tau) \equiv J(t, \tau - t), \quad (12)$$

which means that for every t , $J_T(t, \tau)$ represents the current in the sample at a delay τ after excitation, instead of the current at a delay $t + \tau$. This transformation of

experimental data was introduced by Beard *et al.*⁴ By writing out the convolutions in Eqs. (11) and applying this time-shift transformation, we obtain

$$J_T(t, \tau) = N(\tau)[E_0(t) * j_0(t)], \quad (13a)$$

$$J_T(t, \tau) = E_0(t) * [N(\tau - t)j_0(t)]. \quad (13b)$$

(Note that one should correct $E(t)$ and $E_0(t)$ for the frequency response of the THz detection scheme before applying this time shift.⁴) Now we can calculate the ‘quasiconductivity’

$$\tilde{S}_T(\omega, \tau) \equiv \frac{\mathcal{F}\{J_T(t)\}(\omega)}{\mathcal{F}\{E_0(t)\}(\omega)}. \quad (14)$$

We remind the reader that \tilde{S}_T is a quantity that can be calculated from experimental data, while N and $\hat{\zeta}$ are yet unknown. Applied on the intrinsic-conductivity picture [Eq. (13a)], one would believe that

$$\tilde{S}_T(\omega, \tau) \stackrel{?}{=} N(\tau)\zeta(\omega), \quad (15)$$

i.e. that the quasiconductivity represents the desired conductivity $\sigma(\omega, \tau)$. However, with the time-shift transformation [Eq. (12)], the condition $\tau \gg 0$ for which the intrinsic-conductivity picture is applicable changes into $\tau - t \gg 0$. This new condition is much more restrictive than the old one. If we define the current impulse response time T_{cir} such that $j_0(t) = 0$ for $t > T_{\text{cir}}$, it can be shown that the quasiconductivity $\tilde{S}_T(\omega, \tau)$ is equivalent to the conductivity $\sigma(\omega, \tau)$ only if

$$\tau > T_{\text{cir}}. \quad (16)$$

We now consider the conductivity-with-population picture, which does not have restrictions such as in Eq. (16). Here, we can safely write the quasiconductivity as

$$\begin{aligned} \tilde{S}_T(\omega, \tau) &= \mathcal{F}\{N(\tau - t)j_0\} \\ &= \mathcal{F}\{N(\tau - t)\} * \hat{\zeta}(\omega), \end{aligned} \quad (17)$$

which is independent of the THz pulse shape $E_0(t)$, but does not have a straightforward physical meaning such as Eq. (7). In order to obtain the ‘true’ conductivity $\hat{\sigma}(\omega, \tau)$ in this picture, we must apply a number of additional transformations,

$$S_T(t, \tau) \equiv \mathcal{F}^{-1}\{\tilde{S}_T(\omega, \tau)\}(t) = N(\tau - t)j_0(t) \quad (18)$$

$$S(t, \tau) \equiv S_T(t, \tau + t) = N(\tau)j_0(t) \quad (19)$$

$$\tilde{S}(\omega, \tau) \equiv \mathcal{F}\{S(t, \tau)\}(\omega) = N(\tau)\hat{\zeta}(\omega). \quad (20)$$

Clearly, in the conductivity-with-population picture,

$$\hat{\sigma}(\omega, \tau) = \tilde{S}(\omega, \tau). \quad (21)$$

However, there is a catch, which becomes more obvious from the expansion

$$\begin{aligned} \tilde{S}(\omega, \tau) &= \\ \frac{1}{2\pi} \int_{-\infty}^{\infty} d\omega' \int_{-\infty}^{\infty} d\tau' e^{i(\omega - \omega')(\tau' - \tau)} \tilde{S}_T(\omega', \tau') \end{aligned} \quad (22)$$

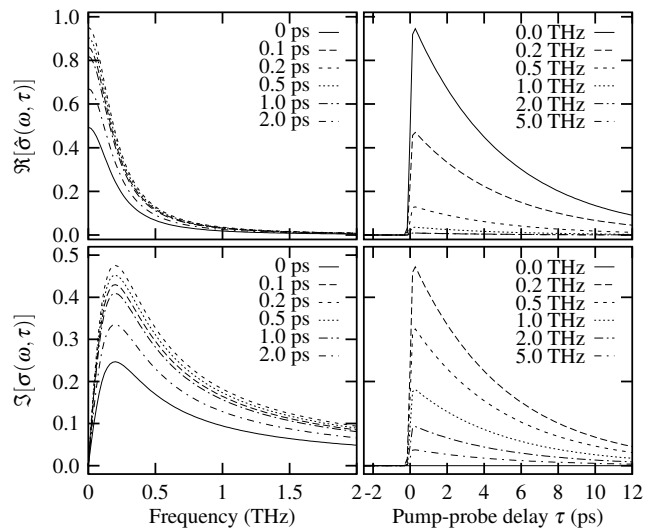


FIG. 3: Model of $\hat{\sigma}(\omega, \tau)$ (in arbitrary units) used for the simulations, here with Drude time constant $\hat{\tau}_D = 0.8$ ps and population relaxation time $\tau_R = 5$ ps. Shown are the real and imaginary components, on the left-hand side for various values of τ and on the right-hand side for various values of $\omega/2\pi$.

of Eqs. (18)–(20), which shows that in order to evaluate $\tilde{S}(\omega, \tau)$ at any particular frequency ω and pump-probe delay τ , one needs full knowledge of $\tilde{S}_T(\omega, \tau)$ at all other frequencies and delays. Because of the limited bandwidth of the THz pulse, this is generally not the case, since Eq. (14) is undefined for $E_0(\omega) = 0$. In the next section, we will test how this limitation, and the limitation [Eq. (16)] of the intrinsic-conductivity picture would affect the analysis of experimental data under various realistic conditions.

V. SIMULATIONS

Although we have mentioned some possible complications in evaluating the time-dependent conductivity from an experiment, the reverse is not true. One can simulate an experiment from a known model in the conductivity-with-population picture by going backwards from Eq. (21); one only needs to know the shape $E_0(t)$ of the THz pulse. As a test case, we used the Drude model [Eq. (2)], with a number density $N(\tau)$ that is created rapidly, followed by an exponential decay due to recombination with a time constant τ_R ; furthermore we assume that the charge carriers are created instantaneously by an excitation pulse with an FWHM of 0.2 ps. The time constant $\hat{\tau}_D$ is in the conductivity-with-population picture, which relates to the intrinsic-conductivity picture as $\hat{\tau}_D^{-1} = \tau_D^{-1} + \tau_R^{-1}$. Figure 3 shows the model for the conductivity $\hat{\sigma}(\omega, \tau)$ on which the simulations are based.

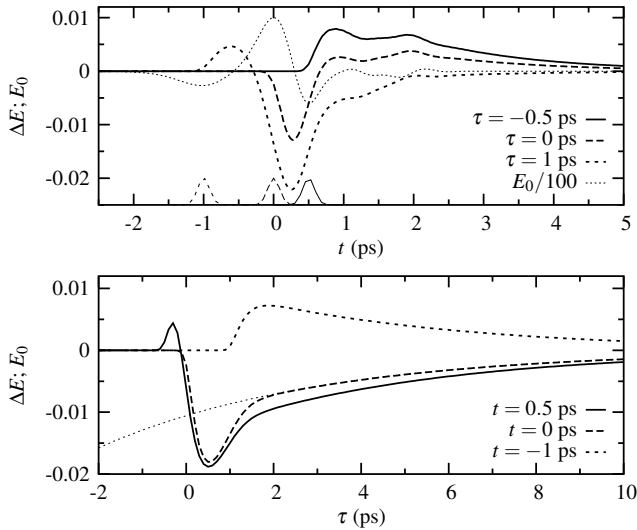


FIG. 4: Simulation of a measurement of the differential signal $\Delta E = E(t, \tau) - E_0(t)$ with the parameters as in Fig. 3. Note that ΔE is a measure for the current density J in the sample. *Upper panel*: the simulated differential signals for various values of the pump-probe delay τ . The small pulse shapes indicate the time overlap between the pump pulse and the THz pulse around $t = -\tau$. Only the part of the THz pulse with $t > -\tau$ is affected by the pump pulse. *Lower panel*: differential signals taken at various t values as a function of τ . The time-shift transformation [Eq. (12)] amounts to aligning the curves in the lower panel. Note the non-exponential decay of the signals for $\tau < 2$ ps; the dotted curve is an exponential function with a time constant of 5 ps.

A. Simulation of time-domain data

First, we simulated an experiment on a sample which has a time-dependent conductivity as shown in Fig. 3, yielding the simulated measurement shown in Fig. 4. As expected, only the part of the THz pulse that passed through the sample after the pump pulse is affected. In a number of publications, not the full two-dimensional signal $\Delta E(t, \tau)$ is measured, but rather the one-dimensional signal $\Delta E(\tau)$ at a fixed gate delay t .^{7,8,11,20,21} Examples of such signals are shown in the bottom panel. Concentrating on the curve for $t = 0$ ps, corresponding to the main peak of the THz pulse, we observe that the signal $\Delta E(t, \tau)$ decays exponentially for $\tau > 2$ ps, while the decay is strongly non-exponential for $\tau < 2$ ps, even though the model exclusively deals with exponentially decaying populations and currents.

The cause for this deviation is that for $\tau < 2$ ps, the excitation pulse overlaps with an earlier part of the THz pulse. This earlier part of the pulse, with a negative amplitude, leads to a negative response which persists for some time and partially cancels the positive response from the central peak of the THz pulse. As can be expected, the non-exponential behavior turns out to be strongly dependent on the THz pulse shape (data not shown). Also, this effect is stronger for larger values of

τ_D in the model: a long-lived impulse response current $\hat{j}_0(t)$ means that the electrical field in the early parts of the THz pulse has a larger influence on the signal later on. This simulation clearly indicates that one must be very careful when interpreting fixed- t traces for τ values which correspond to time overlap with earlier parts of the THz pulse.

If one chooses to use the one-dimensional type of measurements as discussed here, it is recommended that one does not use pulses generated by optical rectification, since these typically start with a long negative prepulse followed by a shorter main pulse. A better choice would be to use pulses generated by photoconductive antennas, which start with a short high-amplitude pulse, followed by a slow negative tail. Since this pulse shape does not have a negative ‘head’, the artifacts discussed above would be much smaller.

B. Evaluation of analysis methods

In this section, we will attempt to extract the quasi-conductivity $\tilde{S}_T(\omega, \tau)$ and conductivity-with-population conductivity $\tilde{S}(\omega, \tau)$ from the simulated experimental data shown in Fig. 4. We will compare these quantities to the model in Fig. 3 on which the simulations were based.

First we will consider the quasiconductivity $\tilde{S}_T(\omega, \tau)$. We mentioned in Section IV that this quantity [see Eq. (14)] represents the conductivity in the intrinsic-conductivity picture, but only under the condition in Eq. (16). Figure 5 shows what happens if it is evaluated from the simulated measurement in Fig. 4. As can be expected from Eq. (17), there is little resemblance between the model in Fig. 3 and $\tilde{S}_T(\omega, \tau)$. If one were to interpret this quantity as the time-dependent conductivity $\sigma(\omega, \tau)$, one might be misled into believing that photoexcitation leads to complicated dynamics in the sample. However, we note that for $\tau \geq 5$ ps, there is reasonable similarity between the underlying model and the quasiconductivity $\tilde{S}_T(\omega, \tau)$, because the condition in Eq. (16) is met. We can see this in the decay of the signal in the upper panel in Fig. 4, which has mostly decayed for $t > 5$ ps.

In this simulation, we assumed that $\tau_D = 0.8$ ps, which resulted in a current impulse response duration $T_{\text{cir}} \approx 5\tau_D$. We can compare this to measured values in other studies. In doped silicon, $\tau_D \approx 0.4$ ps,¹⁶ meaning $T_{\text{cir}} \approx 2.5$ ps. In nanocrystalline TiO₂, a non-Drude current impulse response function was shown¹³ that would require $\tau > 0.4$ ps. In bulk GaAs, a modified-Drude model had a time constant $\tau_D \approx 0.16$ ps,⁴ which requires $\tau > 1$ ps. One needs to be very careful in the evaluation of the conductivity within a time T_{cir} after excitation.

Now we will consider the conductivity-with-population conductivity $\tilde{S}(\omega, \tau)$, which can be evaluated from the quasiconductivity. Although the latter has no direct physical meaning, it can be evaluated directly from experimental data and it is indeed independent of the shape

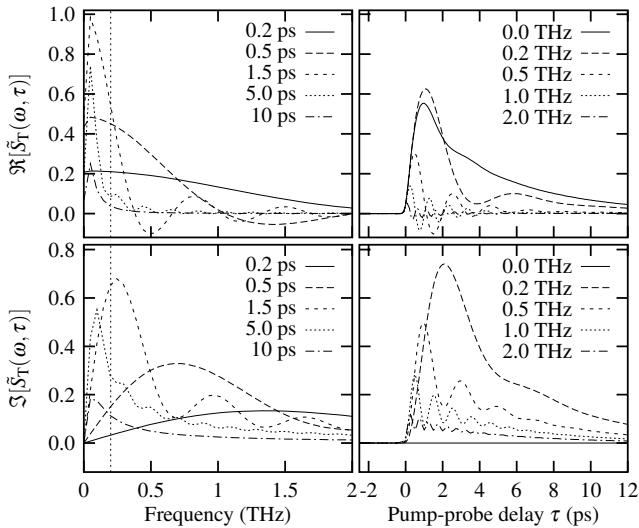


FIG. 5: The real and imaginary components of the quasiconductivity $\tilde{S}_T(\omega, \tau)$ [Eq. (14)] for the model in Fig. 3. Clearly, as could be expected, there is little resemblance between this quantity and the model $\hat{\sigma}(\omega, \tau)$ for pump-probe delays τ below 5 ps. The apparent dynamics are artifacts inherent to the definition of \tilde{S}_T . Note that in a realistic THz experiment, the frequency range below 0.2 THz, left of the vertical lines, would not be available.

of the THz pulses (simulations not shown), which means that it only depends on the properties of the charge carriers in the sample. Due to the bandwidth of the THz pulses, \tilde{S}_T is only known for a limited frequency range [see Eq. (14)]. In order to evaluate \tilde{S} , we must somehow guess the unknown frequency components in the quasiconductivity \tilde{S}_T . As a first test, we assumed that \tilde{S} was known for the frequency range of 0–3 THz, which we extrapolated to higher frequencies with the power laws ω^{-2} for the real part and ω^{-1} for the imaginary part. These power laws correspond to the behavior of the Drude model in Eq. (2). As can be seen from the curves in Fig. 5, this extrapolation is not likely to be very accurate. However, it is a better option than simply padding with zeroes. The result is shown in Fig. 6 and closely resembles the underlying model in Fig. 3. It turns out that missing high-frequency data has a minor impact on the reconstruction.

In a realistic THz experiment, the bandwidth is limited at both the higher and the lower frequencies. For THz pulses generated and detected in ZnTe crystals,³ a typical range is 0.2–2 THz. From a glance at Fig. 5, it will be clear that extrapolating to lower frequencies is not trivial. We chose to pad the lower frequencies with a constant value. Figure 7 shows the result of converting the extrapolated quasiconductivity $\tilde{S}_T(\omega, \tau)$ data to $\tilde{S}(\omega, \tau)$. Clearly, the missing low-frequency data has a huge impact on the result, although it still bears more resemblance to the underlying model in Fig. 3 than the quasiconductivity \tilde{S}_T in Fig. 5. Especially the frequency

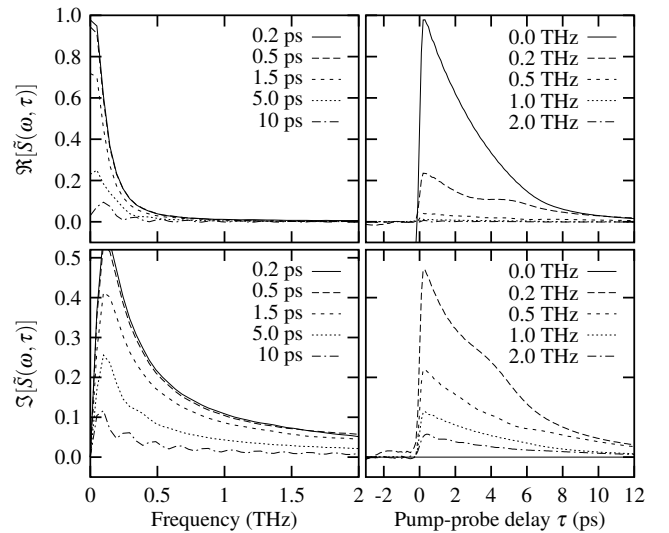


FIG. 6: The real and imaginary components of $\tilde{S}(\omega, \tau)$ [Eq. (20)], again for the model in Fig. 3. In calculating \tilde{S} from \tilde{S}_T , only the frequency range 0–3 THz was used. Higher frequencies were extrapolated as a power law. This reconstructed data closely resembles the underlying model in Fig. 3.

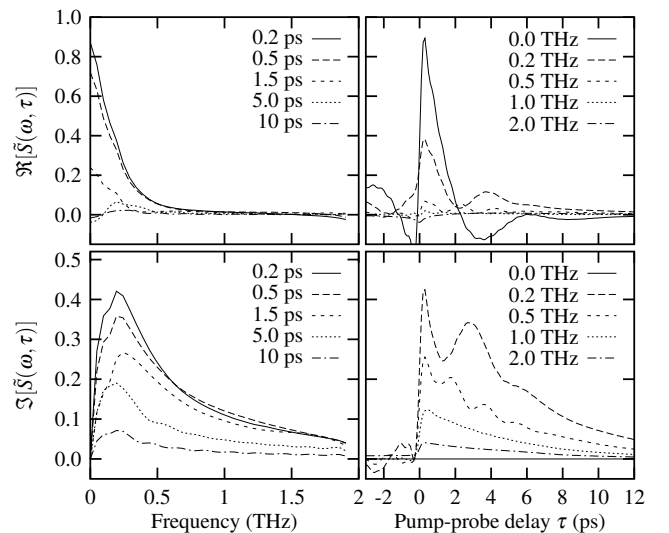


FIG. 7: As in Fig. 6, but based on the quasiconductivity in the frequency range 0.2–2 THz. The missing low- and high-frequency data were extrapolated by a constant and a power law, respectively. Due to the missing low-frequency data, this reconstruction deviates significantly from the underlying model in Fig. 3.

dependence matches reasonably well; the largest differences are found in the τ -dependence. Other extrapolation methods (straight line, smooth transition to zero at $\omega = 0$, or padding with zeroes) gave similar or worse results.

Summarizing, the quasiconductivity $\tilde{S}_T(\omega, \tau)$ can be evaluated from the experimental data and represents the conductivity $\sigma(\omega, \tau)$ in the intrinsic-conductivity picture,

but only for pump–probe delays τ that are much larger than the current impulse response time. The quantity $\tilde{S}(\omega, \tau)$ would represent the conductivity $\hat{\sigma}$ in the conductivity-with-population picture, but can generally not be evaluated from experimental data due to the limited bandwidth of THz pulses. However, it is possible to calculate the measurable quantity $\tilde{S}_T(\omega, \tau)$ from a given model $\hat{\sigma}(\omega, \tau)$. Hence, if a reasonable model for $\hat{\sigma}$ exists, it is in principle straightforward to fit this model to the experimental data.

VI. CONCLUSION

We have presented a formalism which can be used to describe optical pump, THz probe measurements on systems in which the frequency-domain conductivity changes rapidly with time τ after optical excitation. In this description, we use the conductivity $\hat{\sigma}(\omega, \tau)$, in the so-called conductivity-with-population picture. In its frequency dependence, it incorporates both the kinetics of the response of the charge carriers to an electrical field and the recombination dynamics which leads to charge carriers disappearing from the system. Any conductivity model that can be expressed in the form $\hat{\sigma}(\omega, \tau)$ can be tested against experimental data.

In the alternative intrinsic-conductivity picture, the frequency dependence of the conductivity $\sigma(\omega, \tau)$ does not incorporate population dynamics. It can be reconstructed from experimental data, but only for delay values τ that are large compared to the charge-carrier response time. For smaller delay values, the analysis creates artifacts which could be erroneously interpreted as dynamics in the sample.

Even if one is not interested in measuring a frequency-resolved conductivity, one needs to be careful when interpreting transmittance changes in the sample as measured by the central peak of a THz pulse. The exact time profile of the THz pulse can strongly affect such measurements, again especially when the charge-carrier response time is long compared to the duration of the central peak in the THz pulse.

Acknowledgements

This work was financially supported by grants from the Wenner-Gren Foundation and the Crafoord Foundation.

APPENDIX A: DERIVATION OF CURRENT FROM THE MEASURED FIELDS

In this appendix, we will derive Eq. (3). Consider the geometry and quantities in Fig. 8. For this geometry, the Maxwell equations can be written as

$$\epsilon_{\text{rel}}(z) \frac{\partial^2}{\partial t^2} E(z, t) + c^2 \frac{\partial^2}{\partial z^2} E(z, t) = \frac{1}{\epsilon_0} J(z, t), \quad (\text{A1})$$

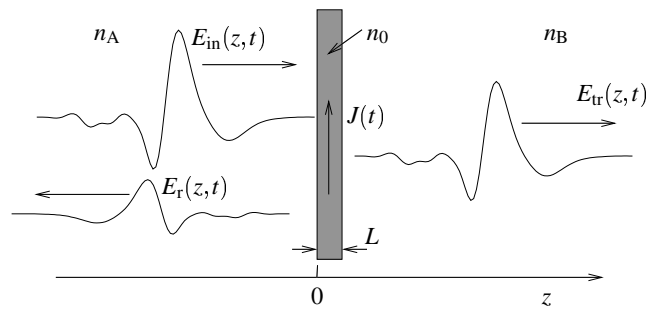


FIG. 8: Geometry of a sample, with an incoming plane-wave THz pulse E_{in} , a reflected pulse E_r , and a transmitted pulse E_{tr} . The field of the THz pulse creates a current density J in a thin sample with thickness L and refractive index n_0 (only relevant for thick samples). The sample is surrounded by materials a and b with refractive indices n_A and n_B . The spatial coordinate is z and the sample is located at $z = 0$.

where ϵ_{rel} is the relative dielectric constant of the medium. Notice that the analysis of pump–probe measurements is greatly complicated if reflections of the THz pulse overlap with the main pulse. Since the refractive index at THz frequencies typically is larger than at optical wavelengths, and one measures the field E instead of the intensity (E^2), a THz pulse that has been reflected twice at the sample substrate boundaries usually has a significant amplitude. Therefore, it is recommended that samples and sample substrates are either thick enough ($L > 1$ mm) to separate the reflections in time, or so thin that the reflection completely overlaps ($L < 10$ μm). We will discuss these two cases separately.

1. Thin samples

In the limit for $L \rightarrow 0$, we can write

$$J(z, t) = L J(t) \delta(z). \quad (\text{A2})$$

We assume that in the mediums surrounding the sample, the refractive index is frequency-independent and the THz absorption can be neglected, i.e. $\epsilon_{\text{rel}} = n^2$. This means that the THz pulses can be described as wave packets, i.e., $E_{\text{in}}(z, t) = A_{\text{in}}(t - zn_A/c)$, $E_r(z, t) = A_r(t + zn_A/c)$, and $E_{\text{tr}}(z, t) = A_{\text{tr}}(t - zn_B/c)$, where $A_{\text{in}}(t)$ defines the incoming pulse shape and $A_r(t)$ and $A_{\text{tr}}(t)$ are not yet known. Hence, we write

$$E(z, t) = \begin{cases} A_{\text{in}}(t - zn_A/c) + A_r(t + zn_A/c) & (z < 0) \\ A_{\text{tr}}(t - zn_B/c) & (z > 0) \end{cases}. \quad (\text{A3})$$

By substituting Eqs. (A2) and (A3) into Eq. (A1), and the boundary condition that E is continuous at $z = 0$, we can obtain

$$J(t) = \frac{\epsilon_0 c}{L} [2n_A A_{\text{in}}(t) - (n_A + n_B) A_{\text{tr}}(t)]. \quad (\text{A4})$$

In the derivation, we have assumed that $J(-\infty) = 0$ and $A_{\text{in}}(-\infty) = 0$, i.e., there was neither a current nor a field

present before the THz pulse arrived. In a THz transmittance measurement, we compare A_{tr} with a conductive sample ($J \neq 0$) to the field A_{tr}^0 with a nonconductive sample ($J = 0$). Hence,

$$J(t) = \frac{\epsilon_0 c (n_A + n_B)}{L} [A_{\text{tr}}^0(t) - A_{\text{tr}}(t)], \quad (\text{A5})$$

which is equivalent to Eq. (3).

2. Thick samples

In thick samples, the index of refraction n at depth z in the sample is given by

$$n^2 = n_0^2 \left(1 + i \frac{\sigma(z)}{\omega \epsilon_0 n_0^2} \right), \quad (\text{A6})$$

where n_0 is refractive index in the absence of charge carriers. We use the sign conventions imposed by Eq. (1). If we assume that the second term is small, and we ignore multiple reflections, but take absorption losses into account, as well as reflection losses at the sample boundaries, then we can derive that

$$\frac{A_{\text{tr}}}{A_{\text{tr}}^0} - 1 = \frac{1}{2\omega\epsilon_0 n_0^2} \left(-\frac{n_0\omega}{c} \int_0^L \sigma(z) dz + iR \right) + \mathcal{O}(\sigma^2), \quad (\text{A7})$$

where the first term represents the absorption and

$$R = \sigma(0) \left(\frac{1}{2} - \frac{n_0}{n_0 + n_A} \right) + \sigma(L) \left(\frac{1}{2} - \frac{n_0}{n_0 + n_B} \right) \quad (\text{A8})$$

represents the reflection losses at the sample boundaries. (Reflection losses due to variations of $\sigma(z)$ within the sample are $\mathcal{O}(\sigma^2)$ and can be ignored).

If we wish to calculate the current from a measurement, we need to make assumptions about the z dependence of $\sigma(z)$. For example, if there is no z dependence, then

$$\frac{A_{\text{tr}}}{A_{\text{tr}}^0} - 1 = \frac{\sigma}{2\omega\epsilon_0 n_0^2} \left(-\frac{n_0\omega L}{c} + iR' \right), \quad (\text{A9})$$

$$R' = 1 - \frac{n_0}{n_0 + n_A} - \frac{n_0}{n_0 + n_B}. \quad (\text{A10})$$

If $n_0 = n_A = n_B$ and σ or if the sample is sufficiently thick (e.g., 1 mm), we can approximate $R \approx 0$ and obtain

$$J \approx -\frac{2\epsilon_0 c n_0}{L} [A_{\text{tr}}^0 - A_{\text{tr}}], \quad (\text{A11})$$

where we used $J = \sigma A_{\text{in}}$. This equation is very similar to Eq. (3), but applies to a steady state. It can be applied to a time-dependent conductivity, but only under the condition that the excitation pulse that creates charge carriers has the same group velocity as the THz pulse. Under this condition, the THz pulse will meet charge carriers that all have the same age while it passes through the sample.

* Electronic address: V.sundstrom@chemphys.lu.se

- ¹ C. A. Schmuttenmaer, Chem. Rev. **104** (2004).
- ² M. C. Beard, G. M. Turner, and C. A. Schmuttenmaer, J. Phys. Chem. B **106**, 7146 (2002).
- ³ M. C. Beard, G. M. Turner, and C. A. Schmuttenmaer, Phys. Rev. B **62**, 15764 (2000).
- ⁴ M. C. Beard, G. M. Turner, and C. A. Schmuttenmaer, J. Appl. Phys. **90**, 5915 (2001).
- ⁵ M. C. Beard, G. M. Turner, and C. A. Schmuttenmaer, Nano Lett. **2** (2002).
- ⁶ M. C. Beard, G. M. Turner, J. E. Murphy, O. I. Micic, M. C. Hanna, A. J. Nozik, and C. A. Schmuttenmaer, Nano Lett. **3** (2003).
- ⁷ D. G. Cooke, F. A. Hegmann, Y. I. Mazur, W. Q. Ma, X. Wang, Z. M. Wang, G. J. Salamo, M. Xiao, T. D. Mishima, and M. B. Johnson, Appl. Phys. Lett. **85** (2004).
- ⁸ F. A. Hegmann, R. R. Tykwinski, K. P. H. Lui, J. E. Bullock, and J. E. Anthony, Phys. Rev. Lett. **89**, 227403 (2002).
- ⁹ E. Hendry, J. M. Schins, L. P. Candéias, L. D. A. Siebbeles, and M. Bonn, Phys. Rev. Lett. **92**, 196601 (2004).
- ¹⁰ E. Hendry, M. Koeberg, J. M. Schins, H. K. Nienhuys, V. Sundström, L. D. A. Siebbeles, and M. Bonn, Phys. Rev. B **71**, 125201 (2005).
- ¹¹ P. U. Jepsen, W. Schaier, I. H. Libon, U. Lemmer, N. E. Hecker, M. Birkholz, K. Lips, and M. Schall, Appl. Phys. Lett. **79**, 1291 (2001).
- ¹² C. Messner, H. Kostner, R. A. Hopfel, and K. Unterrainer, J. Opt. Soc. Am. B **18**, 1369 (2001).
- ¹³ G. M. Turner, M. C. Beard, and C. A. Schmuttenmaer, J. Phys. Chem. B **106**, 11716 (2002).
- ¹⁴ J. T. Kindt and C. A. Schmuttenmaer, J Chem Phys **110**, 8589 (1999).
- ¹⁵ H. Nemeč, F. Kadlec, and P. Kuzel, J. Chem. Phys. **117**, 8454 (2002).
- ¹⁶ T. I. Jeon and D. Grischkowsky, Phys. Rev. Lett. **78**, 1106 (1997).
- ¹⁷ W. Zhang, A. K. Azad, and D. Grischkowsky, Applied Physics Letters **82**, 2841 (2003).
- ¹⁸ A. S. Vengurlekar and S. S. Jha, Physical Review B **43**, 12454 (1991).
- ¹⁹ N. W. Ashcroft and N. D. Mermin, *Solid State Physics* (Saunders College Publishing, 1976).
- ²⁰ M. Schall and P. U. Jepsen, Applied Physics Letters **80**,

4771 (2002).
²¹ V. K. Thorsmølle, R. D. Averitt, X. Chi, D. J. Hilton, D. L. Smith, A. P. Ramirez, and A. J. Taylor, Applied Physics

Letters **84**, 891 (2004).